# **Dynamic Control of Spring-driven Mechanisms**

Abstract: A common method for moving a machine member from one position to another is the use of a spring. Spring-driven devices are simple, inexpensive, and easy to implement; however, the velocity characteristics of such devices leave much to be desired. The velocity increases from the initial position to the final position resulting in a maximum velocity, and therefore maximum energy in the mechanism, at the final position. The simplest method of stopping the device, a rigid stop, results in high impact forces and undesirable noise. Many methods have been developed for limiting the velocity of spring-driven mechanisms, such as the centrifugal friction brakes used in telephone dials and fans used in music boxes. Other approaches such as dashpots or shock absorbers have been used to decelerate devices. This paper discusses a method for both velocity control and deceleration by the use of a single pneumatic cylinder. In addition, a method of reducing velocity variability due to differences among the work functions of the mechanism is described, and the application of such a device to a paper-cutting mechanism is presented. The concepts and theory presented are general and therefore apply to the entire class of spring-driven mechanisms.

#### Introduction

The use of air cylinders to limit velocity is quite common (e.g., door-closing devices). Because of the familiarity of these devices and their apparent simplicity, it is easy to assume that by merely selecting a cylinder diameter and experimentally determining orifice placement and size, one can easily define a satisfactory controlling device. Actually, the problem is deceptively complex because of the dynamic action of the air, which can make the device nearly conservative, dissipative, or any combination of these conditions. The investigation of these dynamic effects by the use of a mathematical model provides insights such that the desirable dynamic effects can be optimized and the undesirable effects neutralized in the design of such a device.

## Nomenclature

- a orifice area (in.²)
- $a_{\rm c}$  compression orifice area (in.<sup>2</sup>)
- $a_{\rm e}$  expansion orifice area (in.<sup>2</sup>)
- A total piston area (in.<sup>2</sup>)
- $A_0$  piston area minus cross-sectional area of piston shaft (in.<sup>2</sup>)
- $A_s$  cross-sectional area of piston shaft (in.<sup>2</sup>)

- B a logic variable containing embedded constants and switches to account for inertia effects of the stationary knife
- C orifice discharge coefficient
- $F_{\rm f}$  friction force (lb)
- F<sub>s</sub> spring force (lb)
- $F_{\rm t}$  paper-cutting force plus friction force (lb)
- $F_{\rm w}$  weight force (lb)
- g acceleration due to gravity (in./s<sup>2</sup>)
- I total mass moment of inertia of rotating knife mechanism (in.-lb-s²)
- $I_k$  mass moment of inertia of rotating knife (in.-lb-s<sup>2</sup>)
- $I_s$  mass moment of inertia of stationary knife (in.-lb-s<sup>2</sup>)
- k ratio of specific heats for a gas (k = 1.4 for air)
- KE kinetic energy (in.-lb)
- m mass (lb)
- $m_{\rm p}$  mass of piston (lb)
- $m_{\rm s}$  mass of spring (lb)
- M moment (in.-lb)
- n exponent for a polytropic compression process
- p pressure (psia)
- p<sub>a</sub> atmospheric pressure (psia)
- $p_c$  pressure on compression side of piston (psia)
- $p_{\rm e}$  pressure on expansion side of piston (psia)
- $p_x$  pressure at exit plane of orifice for sonic flow (psia)

- pressure-proportional friction coefficient for piston 0 seal (lb/psi)
- radius (in.)
- gas constant  $[R = 53.3 (\text{ft-lb/lb-}^{\circ}R) \text{ for air}]$ R
- T temperature (°R)
- $T_{\rm a}$ atmospheric temperature (°R)
- torque (in.-lb) τ
- rotating knife displacement (radians)  $\theta$
- specific volume of gas (in, 3/lb)
- specific volume of air at atmospheric conditions (in.<sup>3</sup>/lb)
- Vvolume of gas (in.3)
- total volume of pneumatic cylinder minus the volume occupied by the piston and shaft (in.3)
- weight of gas (lb) w
- rotating knife velocity (rad/s)

# Theory

# • Basic concepts of velocity control

To illustrate the basic problem of the control of a springdriven device, consider the sketch of the simplest linear motion case shown in Fig. 1. The velocity of the mass is shown at each position for an uncontrolled system in Fig. 1(a). When there is no work done by the mechanism, the velocity increases until the mass strikes the stop. The stop decelerates the mass in an extremely short distance with accompanying high forces and noise. If work is done by the mechanism, the velocity profile is reduced as shown by the dashed curve. The controlled velocity-displacement characteristic in Fig. 1(b) shows three distinct zones: an acceleration zone, a controlledvelocity work zone, and a deceleration zone. The mass is accelerated rapidly (in a short distance to conserve time) to the controlled velocity, is maintained at a uniform velocity for the active-work portion of the stroke, and then is decelerated to a very low velocity in a distance appropriate to the desired deceleration force. To accomplish these desired motions by the addition of a pneumatic control (passive) device is the primary problem considered in this paper. An additional requirement is to have these dynamic characteristics remain relatively constant, even though various work functions are applied and friction forces change over the service life of the device.

# • Pneumatic forces

Consider the pneumatic forces that are generated by the pressure on the piston. Figure 2 illustrates the compression, expansion, and combination modes of operation. Interestingly enough, the compression and expansion modes cause dramatically different dynamic operation. For this reason, the compression and expansion theories are presented separately so that each can be understood

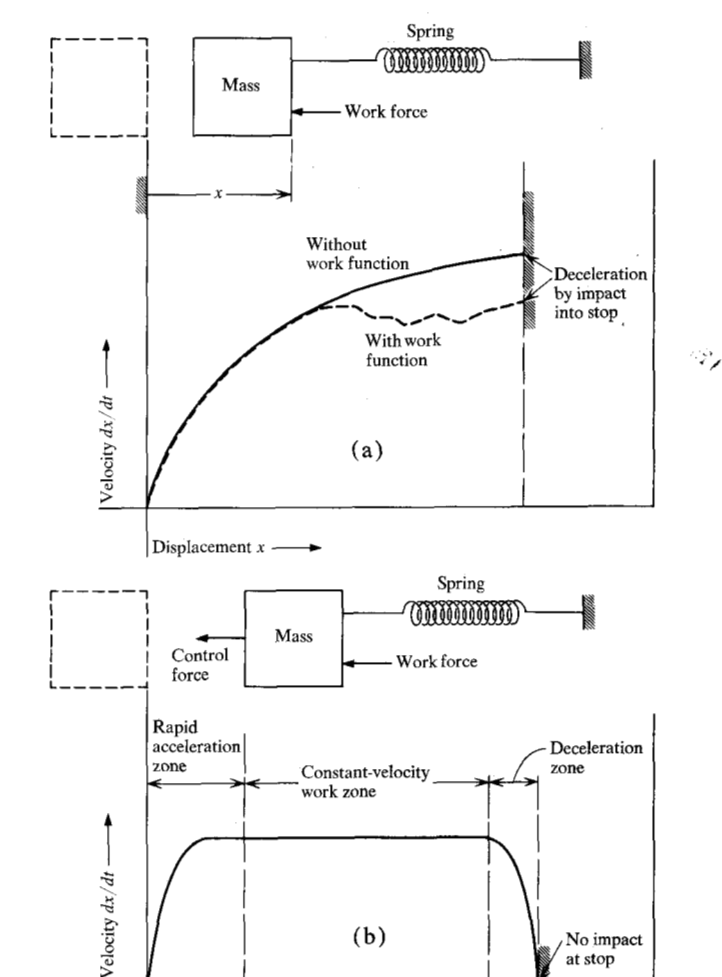


Figure 1 Velocity characteristics of spring-driven device (a) without control and (b) with control of velocity and accelera-

(b)

No impact at stop

and applied in the design to obtain the desired dynamic characteristics.

#### Compression theory\*

Displacement x -

Consider the free-body diagram shown in Fig. 3. The result of summing forces and applying Newton's Second Law is

$$F_{s} + p_{a}A_{o} - p_{c}A_{o} - F_{f} = m(d^{2}x/dt^{2}).$$
 (1)

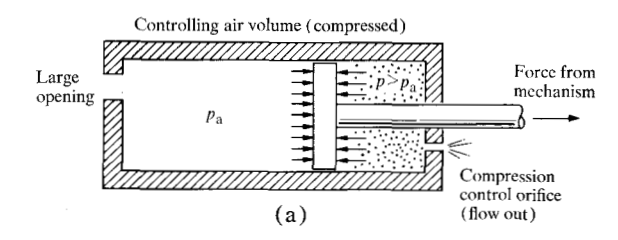
The friction force for the flexible seal in this application has been investigated and found to be proportional to the pressure difference across it, i.e.,

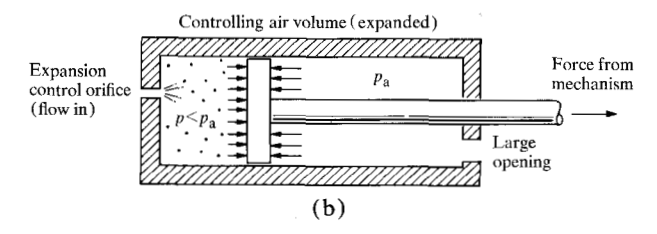
$$F_{\rm f} = Q \left( p_{\rm c} - p_{\rm a} \right) \,. \tag{2}$$

Substituting (2) into (1) yields

$$p_{c} = p_{a} + \frac{F_{s}}{A_{o} + Q} - \left(\frac{m}{A_{o} + Q}\right) \frac{d^{2}x}{dt^{2}}.$$
 (3)

223





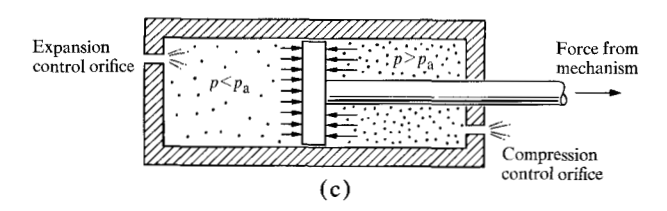


Figure 2 Illustration of pneumatic forces for (a) compression, (b) expansion and (c) combined compression-expansion modes of operation.

The pressure as a function of the thermodynamic properties of air is determined by assuming that the air behaves as a perfect gas, i.e.,

$$pV = wRT. (4)$$

The time rate of change of the pressure is

$$\frac{dp}{dt} = RTV^{-1}\frac{dw}{dt} + RwV^{-1}\frac{dT}{dt} - RwTV^{-2}\frac{dV}{dt}.$$
 (5)

The universal gas constant is

$$R = pV/wT. (6)$$

Substituting (6) into (5) gives

$$\frac{dp}{dt} = \frac{p}{w}\frac{dw}{dt} + \frac{p}{T}\frac{dT}{dt} - \frac{p}{V}\frac{dV}{dt}.$$
 (7)

There are two separate and distinct thermodynamic processes described by Eq. (7). The first term is associated with the flow out of the orifice, which is caused by an adiabatic expansion across the orifice and may be sonic depending upon the pressure ratio. The second and third terms are associated with the change in cylinder pressure from atmospheric to value p. Although this process may be adiabatic, isothermal or any polytropic process between these extremes, the adiabatic assumption was used in this work with accurate results.

The flow through the orifice may be expressed as

$$\frac{dw}{dt} = Ca\left\{ \left(\frac{2gk}{k-1}\right) \frac{p}{\nu} \left[ \left(\frac{p_a}{p}\right)^{2/k} - \left(\frac{p_a}{p}\right)^{(k+1)/k} \right] \right\}^{1/2}$$
 (8)

following Binder's notation [1].

The first term of Eq. (7) is

$$\frac{p}{w}\frac{dw}{dt} = \frac{p}{w}\frac{V}{V}\frac{dw}{dt} = \frac{pv}{V}\frac{dw}{dt}.$$
 (9)

Combining (9) and (8) gives

$$\frac{p}{w}\frac{dw}{dt} = \left(\frac{pv}{V}\right) Ca\left\{2g\frac{p}{v}\left(\frac{k}{k-1}\right) \left[\left(\frac{p_{a}}{p}\right)^{2/k} - \left(\frac{p_{a}}{p}\right)^{(k+1)/k}\right]\right\}^{1/2}$$

or

$$\frac{p}{w}\frac{dw}{dt} = \frac{p}{V}Ca(2gpv)^{1/2}\left\{\left(\frac{k}{k-1}\right)\left[\left(\frac{p_{a}}{p}\right)^{2/k} - \left(\frac{p_{a}}{p}\right)^{(k+1)/k}\right]\right\}^{1/2}.$$
(10)

Assuming a compression process in the cylinder which is polytropic, we may express the term pv in terms of atmospheric conditions as

$$pv = \left(\frac{p}{p_{\rm a}}\right)^{(n-1)/n} p_{\rm a} v_{\rm a}. \tag{11}$$

Substituting (11) into (10) yields

$$\frac{p}{w} \frac{dw}{dt} = \frac{p}{V} \left[ \left( \frac{p}{p_{\rm a}} \right)^{(n-1)/2n} Ca (2gp_{\rm a}v_{\rm a})^{1/2} \right] \times \left\{ \left( \frac{k}{k-1} \right) \left[ \left( \frac{p_{\rm a}}{p} \right)^{2/k} - \left( \frac{p_{\rm a}}{p} \right)^{(k+1)/k} \right] \right\}^{1/2}.$$
(12)

Using the function  $\{F(p)\}\$  for the terms within the outer brackets [ ] to indicate that this is a flow term which is a function of pressure p, we write (12) as

$$\frac{p}{w}\frac{dw}{dt} = \frac{p}{V}\{F(p)\}. \tag{13}$$

Note that all terms in the flow term  $\{F(p)\}$  are constant for sonic flow except the first  $(p/p_a)^{(n-1)/2n}$ , which varies only slightly over a wide range of  $p/p_a$ . (For sonic flow, the pressure ratio  $p_a/p$  is replaced by the constant critical pressure ratio  $p_x/p$ .) Since the flow term  $\{F(p)\}$  is not constant for nonsonic flow (which is important for this application),  $\{F(p)\}$  is carried in its complete form and is not approximated for sonic flow conditions.

The second term in Eq. (7) involves temperature, which can be expressed in terms of pressure by using the pressure-temperature relationship for a polytropic compression process,

$$T = T_{a} \left(\frac{p}{p_{a}}\right)^{(n-1)/n} \tag{14}$$

Taking the time derivative of the natural logarithm of T in Eq. (14) yields

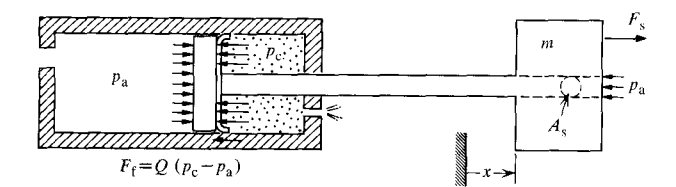


Figure 3 Forces acting on piston in compression mode.



or

$$\frac{p}{T}\frac{dT}{dt} = \left(\frac{n-1}{n}\right)\frac{dp}{dt},\tag{16}$$

which is the second term in Eq. (7),

Now Eqs. (16) and (13) may be substituted into (7), which reduces to

$$\frac{dp}{dt} = \frac{np}{V} \left[ \{ F(p) \} - \frac{dV}{dt} \right],\tag{17}$$

in which

$$\{F(p)\} = -\left[\left(\frac{p}{p_{\rm a}}\right)^{(n-1)/2n} Ca(2gp_{\rm a}v_{\rm a})^{1/2} \times \left\{\left(\frac{k}{k-1}\right)\left[\left(\frac{p_{\rm a}}{p}\right)^{2/k} - \left(\frac{p_{\rm a}}{p}\right)^{(k+1)/k}\right]\right\}^{1/2}\right].$$
(18)

The negative sign for  $\{F(p)\}\$  is necessary so that pressure changes due to flow out of the orifice are compatible with volume increases, which also decrease pressure.

The volume V of air being compressed may be expressed as a function of piston displacement x as

$$V = V_{\mathrm{T}} - A_{\mathrm{o}}x,\tag{19}$$

so that

$$\frac{dV}{dt} = -A_o \frac{dx}{dt}.$$
 (20)

Substituting (19) and (20) into (17) yields an equation for the time rate of change of pressure as a function of piston velocity dx/dt and flow  $\{F(p)\}$ , which is

$$\frac{dp}{dt} = \frac{np}{V_x - A_{xx}} \left[ \left\{ F(p) \right\} + A_0 \frac{dx}{dt} \right]. \tag{21}$$

Equations (21) and (3) are repeated below with the subscript c added to identify these differential equations with the compression mode of operation. The polytropic exponent n has been changed to the specific heat ratio k (k = 1.4 for air) because the rapid compression process inhibits heat transfer and makes the adiabatic compression assumption valid. These differential equations are

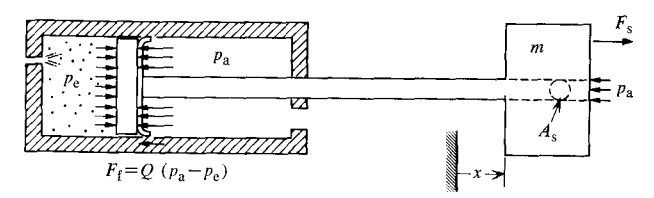


Figure 4 Forces acting on piston in expansion mode.

$$p_{c} = p_{a} + \frac{F_{s}}{A_{o} + O} - \left(\frac{m}{A_{o} + O}\right) \frac{d^{2}x}{dt^{2}},$$
 (3)

and

$$\frac{dp_{\rm c}}{dt} = \frac{np_{\rm c}}{V_{\rm T} - A_{\rm e}x} \left[ \left\{ F(p_{\rm c}) \right\} + A_{\rm o} \frac{dx}{dt} \right],\tag{21}$$

in which

$$\{F(p_{c})\} = -\left[\left(\frac{p_{c}}{p_{a}}\right)^{(k-1)/2k} C a_{c} (2gp_{a}v_{a})^{1/2} \times \left\{\left(\frac{k}{k-1}\right) \left[\left(\frac{p_{a}}{p_{c}}\right)^{2/k} - \left(\frac{p_{a}}{p_{c}}\right)^{(k+1)/k}\right]\right\}^{1/2}\right].$$
(18)

An additional complication that must be considered is caused by the rebound condition that occurs when the orifice is very small and the system is "almost conservative." Under these conditions the air acts like a spring, causing the piston to rebound and subsequently reduce the pressure in the cylinder to below atmospheric pressure. The flow through the orifice reverses, which requires a change in Eq. (21) to describe the condition. Following a similar derivation to the one used to develop Eqs. (18) and (21) yields

$$\frac{dp_{\rm c}}{dt} = \frac{np_{\rm c}}{V_{\rm T} - A_{\rm o}x} \left[ \left\{ F'(p_{\rm c}) \right\} + A_{\rm o} \frac{dx}{dt} \right],\tag{22}$$

in which

$$\{F'(p_{c})\} = \left[ \left( \frac{p_{a}}{p_{c}} \right)^{1/k} C a_{c} (2g p_{a} v_{a})^{1/2} \right] \times \left\{ \left( \frac{k}{k-1} \right) \left[ \left( \frac{p_{c}}{p_{a}} \right)^{2/k} - \left( \frac{p_{c}}{p_{a}} \right)^{(k+1)/k} \right] \right\}^{1/2}.$$
 (23)

Note not only that the sign of  $\{F(p_c)\}$  changes but also that the pressure ratios under the radical are inverted and the exponent of the first term is changed.

## • Expansion mode

The equations describing the expansion mode of operation illustrated in Figs. 2(b) and 4 are derived similarly. The pressure on the expansion side is identified by the subscript e. These differential equations are

$$p_{\rm e} = p_{\rm a} + \frac{F_{\rm s}}{A + Q} + \left(\frac{m}{A + Q}\right) \frac{d^2 x}{dt^2}$$
 (24)

225

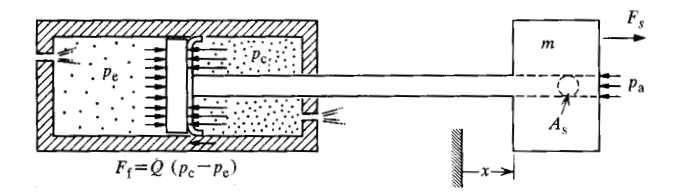


Figure 5 Forces acting on piston in combination mode.

Figure 6 Comparison of dynamic characteristics of (a) compression and (b) expansion modes.

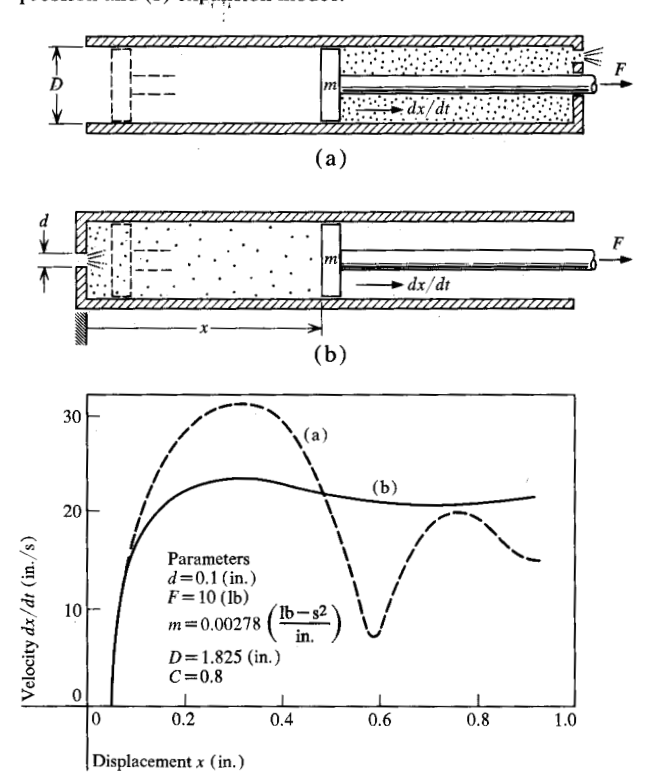
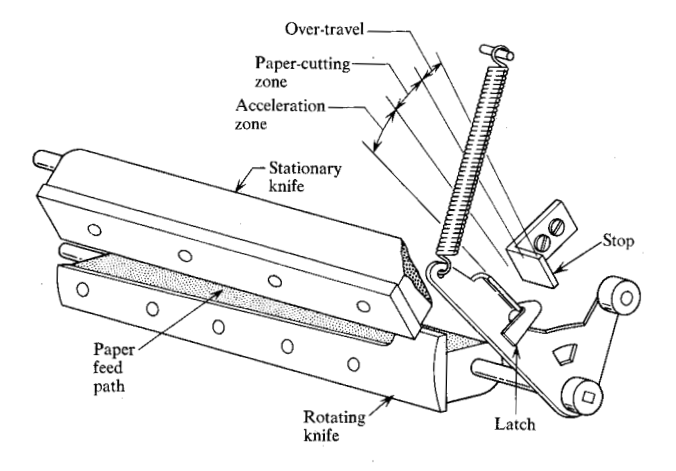


Figure 7 Rotary paper-cutting mechanism.



and

$$\frac{dp_{\rm e}}{dt} = \frac{np_{\rm e}}{Ax} \left[ \left\{ F(p_{\rm e}) \right\} - A \frac{dx}{dt} \right],\tag{25}$$

in which

$$\{F(p_{e})\} = \left[ \left( \frac{pa}{p_{e}} \right)^{1/k} Ca_{e} (2gp_{a}v_{a})^{1/2} \right. \\ \left. \times \left\{ \left( \frac{k}{k-1} \right) \left[ \left( \frac{p_{e}}{p_{a}} \right)^{2/k} - \left( \frac{p_{e}}{p_{a}} \right)^{(k+1)/k} \right] \right\}^{1/2} \right]. \tag{26}$$

The rebound condition can also occur in this mode of operation, and it causes flow out of the orifice if the pressure within the cylinder exceeds atmospheric. This flow expression is

$$\{F'(p_{e})\} = -\left[\left(\frac{p_{e}}{p_{a}}\right)^{(k-1)/k} C a_{e} (2gp_{a}v_{a})^{1/2} \times \left\{\left(\frac{k}{k-1}\right) \left[\left(\frac{p_{a}}{p_{e}}\right)^{2/k} - \left(\frac{p_{a}}{p_{e}}\right)^{(k+1)/k}\right]\right\}^{1/2}\right]. \quad (27)$$

Note that Eqs. (27) and (18) are identical in form since both describe flow out of an orifice to atmospheric pressure just as Eqs. (23) and (26) describe flow into an orifice from atmospheric pressure.

# • Combination mode

The equations describing the combination mode of operation illustrated in Fig. 2(c) are derived by combining the two previous derivations with the exception of the basic force balance. A free-body diagram of the piston and mass illustrated in Fig. 5 yields

$$\frac{d^{2}x}{dt^{2}} = \frac{F_{s}}{m} + p_{e} \left( \frac{A + Q}{m} \right) - p_{c} \left( \frac{A_{o} + Q}{m} \right) - p_{a} \frac{A_{s}}{m}.$$
 (28)

The derivatives of the pressure on the expansion and compression sides of the piston are given by Eqs. (25) and (22), respectively. The simultaneous numerical solution of these equations with Eq. (28) yields the solution of the combination mode of operation.

A very important conclusion about controlling parameters may be reached by studying the compression and expansion solutions separately before combining them. The initial rate of change of pressure with respect to position is inversely proportional to the initial volume on the expansion side. By making this initial volume small, the pressure drop occurs with small motions of the piston, allowing velocity control during the acceleration portion of the motion. This amount of initial controlling air volume is not possible in the compression mode because of the relatively large volume to be compressed. Thus the expansion orifice flow controls the magnitude of the limiting velocity, and the initial expansion volume controls the position at which the velocity is limited.

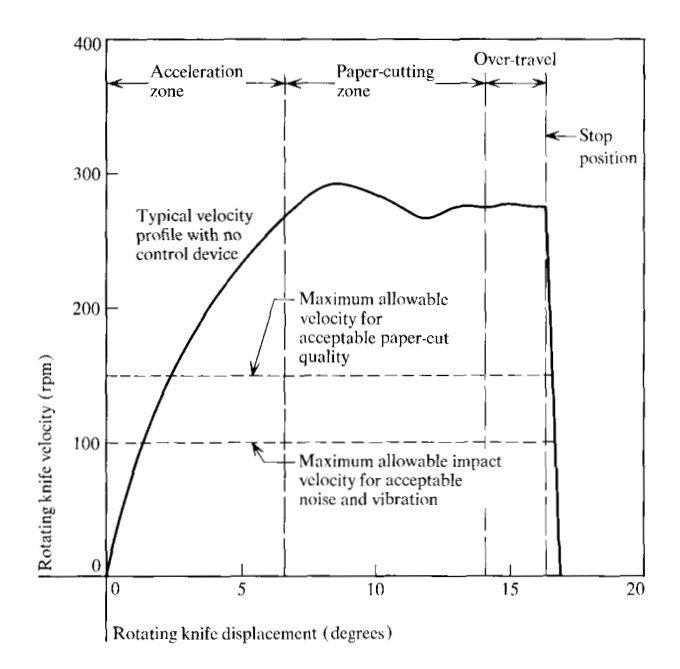


Figure 8 Velocity vs displacement for rotating knife without control. Also shown are velocity requirements for acceptable paper edge quality and stop-impact force reduction.

Computer solutions comparing the expansion and compression modes for equal orifice diameters are shown in Fig. 6. Note the large oscillation that occurs in the compression mode as compared with the smoothness of the expansion mode.

## • Work function theory

With the characteristics of the expansion mode just described, it is obvious that the expansion mode can be used to control the velocity in the acceleration zone and the limiting velocity zone. The compression mode controls the velocity in the deceleration zone. However, the "ideal" constant velocity zone cannot be controlled easily if work is being done. Particularly, if different amounts of work are required, such as cutting the different paper weights described below, the velocity will be controlled by the magnitude of the work function. To alleviate this difficulty, three conditions must be met. First, the spring driving the system must be selected such that the work that it does is much larger than the work function. Second, the piston diameter must be selected so that the pneumatic control can balance the spring work. Third, orifices must be cut in the sides of the cylinder and placed such that the expansion pressure drop is reduced as the piston moves into the work zone and then the compression pressure is generated just prior to the deceleration zone. The orifice placement is described below in the paper-cutting application with the resulting controlling forces.

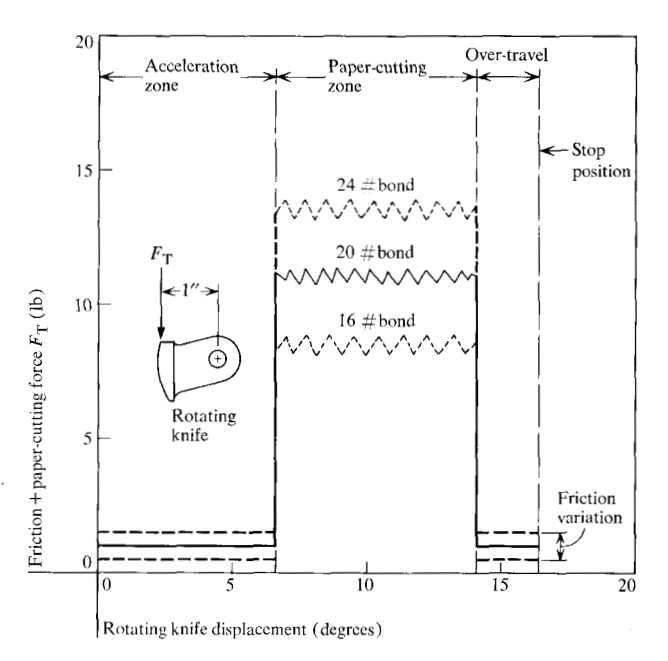


Figure 9 Examples of work-function variation for paper-cutting mechanism and varying weights of paper.

Note that with this approach, this passive pneumatic device can control velocity over a widely varying set of conditions without either initial or field adjustment for changing conditions.

#### Application of theory

This general theory has been applied to design a velocity/deceleration control device for the rotary paper-cutting mechanism shown in Fig. 7. Motion requirements for the rotating knife blade are also shown in the Figure. The existence of three distinct displacement regions directly allowed the application of the above theory. It was found that satisfactory paper edge quality could be obtained over a broad range of knife edge conditions if the rotating knife velocity were limited. Additionally, undesirable noise and vibration could be eliminated by limiting the stop impact velocity of the rotating knife. The actual requirements are shown on the graph of rotating knife velocity vs displacement for the mechanism with no control device in Fig. 8. The maximum time allowed to cut the paper is 0.030 seconds after release of the rotating knife. All of these requirements have to be met while accounting for variations in the weight of the paper and changes in the friction of the mechanism. The range of variations considered is shown on the graph of friction and paper-cutting force vs rotating knife displacement in Fig. 9.

Some idea of the effect of these variations can be obtained by considering the hypothetical case in which a

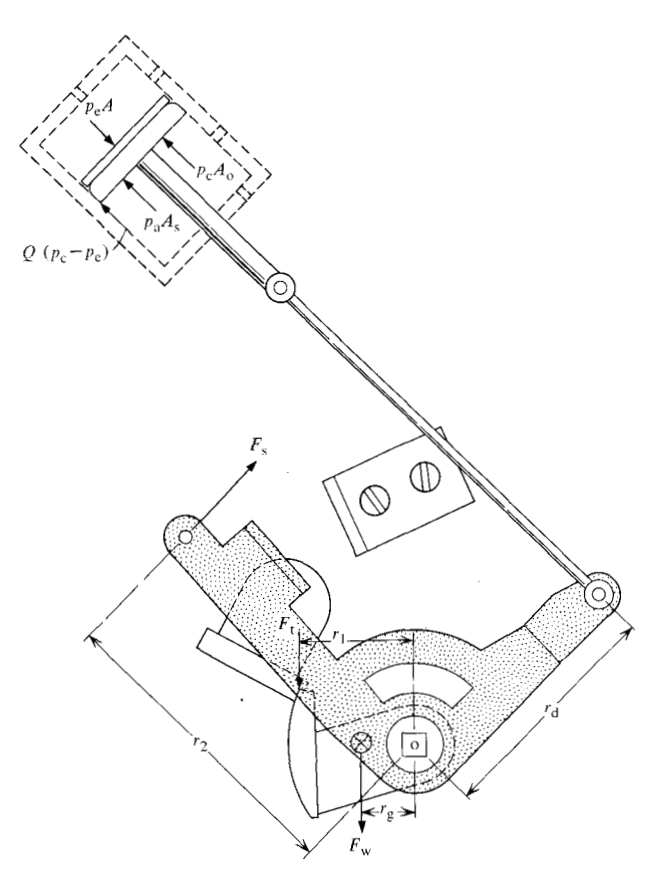
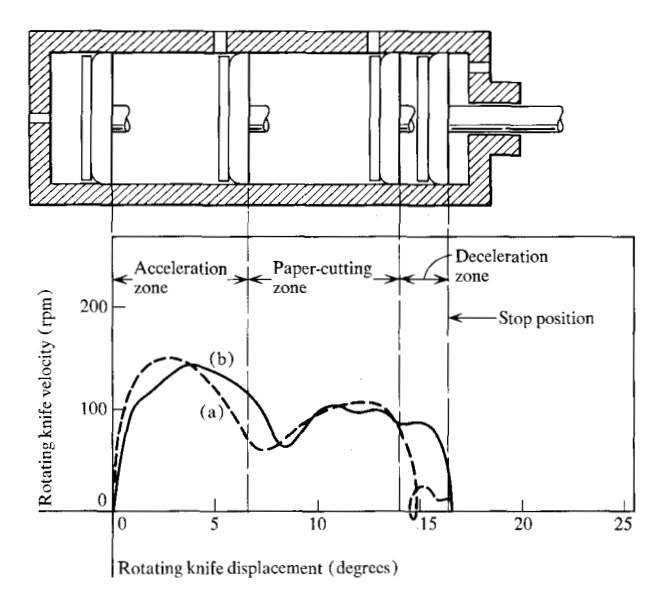


Figure 10 Free-body diagram of paper-cutting mechanism with control device.

Figure 11 (a) Predicted and (b) experimental velocity-vs-displacement curves for rotating knife with control. The drawing shows piston position at each of the transition points of the work function.



spring is designed to provide just enough energy to overcome friction and cut 24-pound bond paper. This condition would require approximately 1.920 in.-lb, as indicated by the area under the force-displacement curve in Fig. 9. The result would be zero rotating knife stop impact velocity, since there would be no energy in the system at the completion of the stroke. However, if one then changed to 16-pound bond paper, the energy required would be only 1.257 in.-lb (also as indicated in Fig. 9). The excess energy available, 0.663 in.-lb, would remain in the system as kinetic energy of the rotating knife to be dissipated upon impact with the stop. The resulting stop impact velocity can be calculated from the following energy equation:

$$KE = \frac{1}{2} I_{\mathbf{k}} \omega^2, \tag{29}$$

where  $\omega = d\theta/dt$ , the rotating knife velocity.

Using the appropriate value for the inertia  $I_k$  (0.002639 in.-lb-s<sup>2</sup>) and taking the kinetic energy to be equal to the excess energy available from the situation above, one obtains a stop impact velocity of 214 rpm! Thus, under such conditions, the stop impact velocity would exceed the allowable limit for eliminating noise and vibration.

With no control device, changes in the required work function energy are reflected directly as changes in the kinetic energy of the mechanism; however, if a control device is used, changes in the required work function energy are manifested as changes in the kinetic energy plus changes in the energy dissipated by the control device. In terms of work done, this relationship can be stated as

$$\int \tau_{s} d\theta - \int \tau_{t} d\theta - \int \tau_{d} d\theta = \Delta K E \tag{30}$$

where  $\tau_s$ ,  $\tau_t$ , and  $\tau_d$  are torques acting on the rotating knife produced by the spring force, the paper-cuttingplus-friction force (work function), and the control device force, respectively. If the available spring energy is increased to a level several times greater than that required by the work function (i.e., if  $\tau_s$  is increased), then the burden of energy removal is placed on the control device. This condition requires a higher effective "damping coefficient" to maintain a given controlled velocity. Thus for a given variation in the required work function energy, a large percentage of the change will be absorbed by the dissipative effects. This result minimizes variations in the kinetic energy (or velocity) of the mechanism due to variations in the work function. Stated another way, small changes in the kinetic energy (or velocity) of the mechanism cause large changes in the dissipation effect produced by the control device. (In the present case, the spring energy was limited by the strength of mechanical elements involved to a level approximately 3.25 times that required to cut 20 pound bond paper and overcome friction.)

#### • Structure of mathematical model and results

Design of the control device was facilitated by the use of a mathematical model. A free-body diagram of the paper-cutting mechanism with control device is shown in Fig. 10. In addition to the active forces shown, an inertia effect of the stationary knife caused by a "scissors" action of the mechanism was taken into account. (The axes of the two knife blades are slightly inclined to insure proper shearing action. As a result, the stationary knife is displaced through a small angle as the rotating knife cuts the paper.) A dynamic friction force produced by the associated inertial reaction was taken into account. The spring force  $F_s$ , the radii  $r_g$  and  $r_g$ , and the combined friction/paper-cutting force  $F_t$  were all described as functions of rotating knife displacement. The lateral orifice areas in the control device were described as step changes in the values of  $a_c$  and  $a_e$  [refer to Eqs. (23) and (27)]. Inertia effects of the piston, connecting linkage, and spring were also included.

Summing moments about point o in Fig. 10 and applying the principle of angular momentum for small displacements, one obtains

$$\sum M_0 = \frac{d}{dt} \left( I \frac{d\theta}{dt} \right) = I \frac{d^2 \theta}{dt^2}$$
 (31)

where

$$\sum M_{\rm o} = F_{\rm s} r_{\rm 2} - F_{\rm w} r_{\rm g} - F_{\rm d} r_{\rm 1} - [p_{\rm c} A_{\rm o} + p_{\rm a} A_{\rm s} + Q(p_{\rm c} - p_{\rm e}) - p_{\rm e} A] r_{\rm d}$$
(32)

and

$$I = I_{k} + BI_{s} + m_{p}r_{d}^{2} + \frac{1}{3}m_{s}r_{s}^{2};$$
(33)

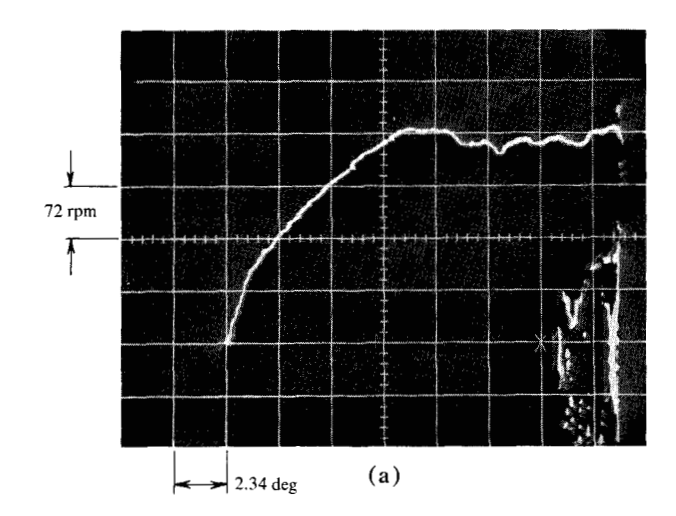
combining (31), (32), and (33), we have

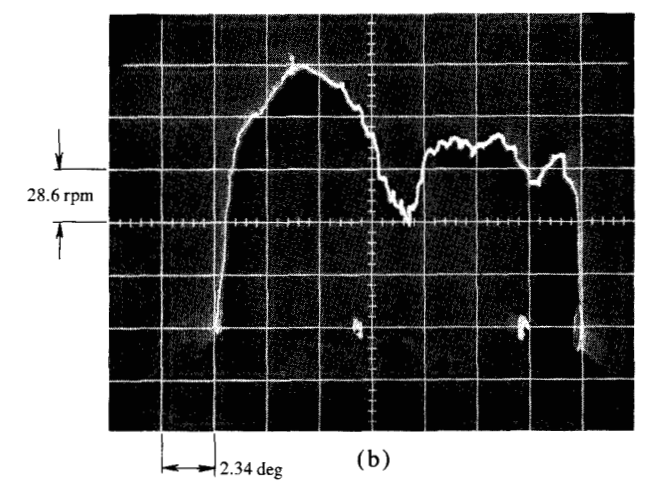
$$\frac{d^{2}\theta}{dt^{2}} = \{F_{s}r_{2} - F_{w}r_{g} - F_{t}r_{1} - [p_{c}A_{o} + p_{a}A_{s} + Q(p_{c} - p_{e}) - p_{e}A]r_{d}\}$$

$$\div (I_{k} + BI_{s} + m_{p}r_{d}^{2} + \frac{1}{3}m_{s}r_{2}^{2}). \tag{34}$$

The pressures  $p_e$  and  $p_e$  are determined by integrating Eqs. (22) and (25), where  $x = r_d\theta$ . The describing equations, (22), (25) and (34), are readily adapted for numerical solution by using the IBM Continuous System Modeling Program (CSMP) [2].

Design iterations using this model were performed on an IBM System/360 Model 50 digital computer to determine appropriate values for orifice size and position. Prototypes were constructed and tested in the laboratory, and experimental results are compared with predicted values in Fig. 11. Experimental dynamic results for the mechanism with and without the control device are shown in Fig. 12. Experimental results showing the effect of variations in paper weight are given in Fig. 13.





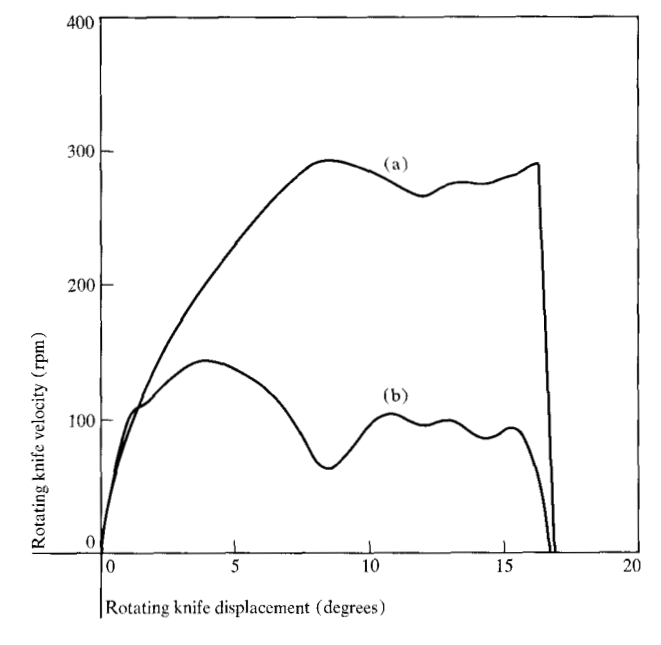


Figure 12 Comparison of experimental results for rotating knife (a) without and (b) with control device. (A larger spring was used on the controlled knife.)

229

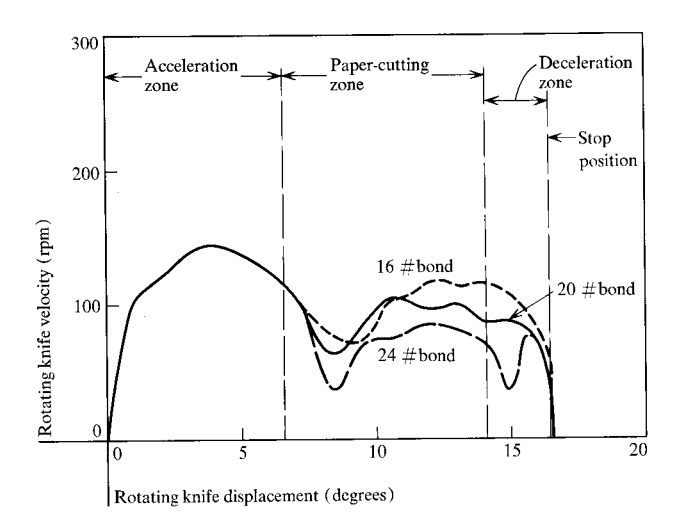


Figure 13 Experimental results for same conditions as in Fig 12(b) showing effects of work function variation on knife velocity.

Note that although the work function changed 0.663 in.lb in going from 16 pound bond paper to 24 pound bond paper, the kinetic energy in the mechanism at the end of paper cut was increased by only 0.120 in.-lb. The time required to cut 24 pound bond paper (worst case) is 0.029 seconds.

#### **Conclusions**

By separating and utilizing the expansion and compression effects of the air cylinder, the proper torque balances have been obtained to effect velocity and deceleration control for the paper-cutting mechanism. The various torques acting on the system with control device are shown in Fig. 14. The expansion mode (controlled by the initial volume and expansion orifice size) determines the initial acceleration characteristics and limiting velocity at the end of the acceleration zone. By increasing the available spring energy and the dissipation capacity of the control device, the burden of energy removal is placed on the control device. This design decision allows the mechanism to tolerate large variations in the work function with no adjustment while meeting stringent velocity requirements in the paper-cutting zone. The deceleration to the stop position is controlled by the compression mode volume (second side orifice position) and the compression orifice diameter, which reduces the kinetic energy at the stop to a negligible amount. The concepts and theory presented herein are general and thus allow a passive, nonadjustable device to control the dynamics of any spring-driven mechanism.

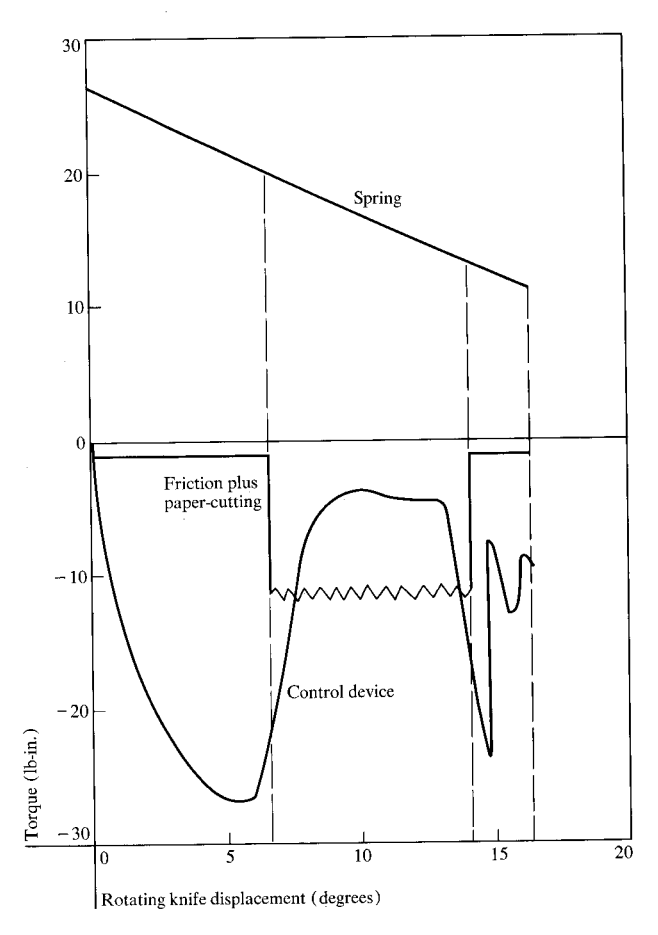


Figure 14 Principal torques on rotating knife.

## **Acknowledgment**

The pneumatic deceleration theory given in this paper is based, in part, on a compression mode deceleration analysis presented in Advanced Dynamical Problems in Machine Design, a graduate course taught by Prof. B. E. Quinn, School of Mechanical Engineering, Purdue University. The authors therefore express their gratitude to Professor Quinn for his very real, though indirect, contribution.

#### References

- R. C. Binder, Fluid Mechanics, 3rd Edition, Prentice-Hall, Inc., Englewood Cliffs, New Jersey 1955, p. 298.
- System/360 Continuous System Modeling Program (360A-CX-16X) User's Manual, IBM Form H20-0367, International Business Machines Corporation (1968).

Received July 7, 1971

The authors are located at the IBM Office Products Division Laboratory, Lexington, Kentucky 40507.